

1 **Effects of ozone-vegetation coupling on surface ozone air**

2 **quality via biogeochemical and meteorological feedbacks**

3 Mehliyar Sadiq¹, Amos P. K. Tai^{1,2}, Danica Lombardozzi³, and Maria Val Martin⁴

4 ¹Graduate Division of Earth and Atmospheric Sciences, Faculty of Science, The Chinese University of Hong
5 Kong, Hong Kong

6 ²Earth System Science Programme, Faculty of Science, The Chinese University of Hong Kong, Hong Kong

7 ³National Center for Atmospheric Research, Boulder, Colorado, USA

8 ⁴Department of Chemical and Biological Engineering, University of Sheffield, Sheffield, UK

9 *Correspondence to:* Amos P. K. Tai (amostai@cuhk.edu.hk)

10

11 **Abstract.** Tropospheric ozone is one of the most hazardous air pollutants as it harms both human health and
12 plant productivity. Foliage uptake of ozone via dry deposition damages photosynthesis and causes stomatal
13 closure. These foliage changes could lead to a cascade of biogeochemical and biogeophysical effects that not
14 only modulate the carbon cycle, regional hydrometeorology and climate, but also cause feedbacks onto surface
15 ozone concentration itself. In this study, we implement a semi-empirical parameterization of ozone damage on
16 vegetation in the Community Earth System Model to enable online ozone-vegetation coupling, so that for the
17 first time ecosystem structure and ozone concentration can coevolve in fully coupled land-atmosphere
18 simulations. With ozone-vegetation coupling, present-day surface ozone is simulated to be higher by up to 4-6
19 ppbv over Europe, North America and China. Reduced dry deposition velocity following ozone damage
20 contributes to ~40-100% of those increases, constituting a significant positive biogeochemical feedback on
21 ozone air quality. Enhanced biogenic isoprene emission is found to contribute to most of the remaining
22 increases, and is driven mainly by higher vegetation temperature that results from lower transpiration rate. This
23 isoprene-driven pathway represents an indirect, positive meteorological feedback. The reduction in both dry
24 deposition and transpiration is mostly associated with reduced stomatal conductance following ozone damage,
25 whereas the modification of photosynthesis and further changes in ecosystem productivity are found to play a
26 smaller role in contributing to the ozone-vegetation feedbacks. Our results highlight the need to consider two-
27 way ozone-vegetation coupling in Earth system models to derive a more complete understanding and yield more
28 reliable future predictions of ozone air quality.

29

30 **1 Introduction**

31 Tropospheric ozone is one of the air pollutants of the greatest concern due to its significant harm to
32 human respiratory health. Increases of ozone since the preindustrial time have been associated with a global
33 annual burden of 0.7±0.3 million respiratory mortalities (Anenberg et al., 2010). Decades of observational
34 records have also demonstrated the damaging effect of surface ozone on vegetation and crop productivity
35 (Ainsworth et al., 2012). The phytotoxicity of ozone is shown to induce stomatal closure and reduce primary
36 production, with ramifications for climate through the modification of surface energy and water fluxes and a
37 decrease in the land carbon sink (Sitch et al., 2007; Wittig et al., 2007; Lombardozzi et al., 2015). Meanwhile,
38 vegetation helps reduce ambient ozone concentration through stomatal deposition (e.g., Kroeger et al., 2014).

39 However, the effect of such ozone-induced vegetation damage on ozone concentration itself, which thereby
40 completes the ozone-vegetation feedback loop, has not been examined before but is potentially significant in
41 modulating tropospheric ozone. This work uses a fully coupled land-atmosphere model to, for the first time,
42 quantify the impacts of ozone-vegetation coupling on surface ozone, and diagnoses the contributions from
43 various feedback pathways in terrestrial ecosystems.

44 Tropospheric ozone is mainly produced from the photochemical oxidation of carbon monoxide (CO),
45 methane (CH₄) and non-methane volatile organic compounds (VOCs) by hydroxyl radical (OH) in the presence
46 of nitrogen oxides (NO_x ≡ NO + NO₂). Vegetation plays various significant roles modulating surface ozone
47 concentration. Precursor gases of ozone have large anthropogenic and natural sources, including vegetation and
48 soil microbes for CH₄ and other VOCs. The most abundant single non-methane VOC species emitted by
49 vegetation is isoprene (C₅H₈), which acts as a major precursor for ozone formation in polluted, high-NO_x
50 regions, but eliminates ozone by direct ozonolysis or by sequestering NO_x as isoprene nitrate in more pristine
51 environments (Fiore et al., 2011). The major sinks for tropospheric ozone include photolysis in the presence of
52 water vapor and uptake by vegetation (i.e., dry deposition, mainly through the leaf stomata). Vegetation,
53 therefore, plays a significant role in modulating ozone biogeochemically through dry deposition and biogenic
54 VOC emissions. Meanwhile, transpiration from vegetation can affect ozone by regulating the overlying
55 hydrometeorological environment. For instance, transpiration influences near-surface water vapor content,
56 which affects the chemical loss rate of ozone. Transpiration also controls surface temperature and mixing depth,
57 which can all influence the formation and dilution of ozone in the atmospheric boundary layer (Jacob and
58 Winner, 2009).

59 Vegetation not only affects but is also affected by surface ozone. Stomatal uptake of ozone by leaves
60 damages internal plant tissues, leading to severe damage to forest, grassland and agricultural productivity
61 (Ashmore, 2005; Karnosky et al., 2007; Ainsworth et al., 2012). Elevated ozone since the industrial revolution is
62 suggested to have reduced light-saturated photosynthetic rate and stomatal conductance by 11% and 13%,
63 respectively (Wittig et al., 2007). Modeling studies have also suggested that elevated ozone could decrease gross
64 primary production (GPP) by 4-8% in the eastern US and more severely so (11-17%) in several hot spots there
65 (Yue and Unger, 2014), and decrease transpiration rate globally by 2-2.4% (Lombardozzi et al., 2015), with
66 significant implications for climate. For instance, the ozone-induced reduction in the global land carbon sink by
67 2100 is shown to have an indirect radiative forcing of +0.62-1.09 W m⁻², which is comparable to the direct
68 radiative forcing of ozone as a greenhouse gas (0.89 W m⁻²) and contributes to more pronounced warming (Sitch
69 et al., 2007). Changes in stomatal conductance also modify the land-atmosphere exchange of water and energy
70 and thus regional hydrometeorology (Bernacchi et al., 2011; Lombardozzi et al., 2015). In view of the important
71 roles vegetation plays in shaping tropospheric ozone, the above biogeochemical and biogeophysical effects
72 induced by ozone damage would affect not only weather and climate but also constitute important feedbacks
73 that ultimately affect ozone air quality itself.

74 In many land surface models, photosynthetic rate and stomatal conductance are highly coupled through
75 the computation within the Farquhar/Ball-Berry model (Farquhar et al., 1980; Ball et al., 1987; Bonan et al.,
76 2011). In global modeling studies on ozone-mediated vegetation changes and climate (Sitch et al., 2007; Collins
77 et al., 2010; Yue and Unger, 2014), the effects of ozone damage on photosynthesis and stomata are thus strongly
78 coupled to each other. Ozone uptake is assumed to directly affect photosynthetic rate, which in turn affects

79 stomatal conductance via changes in internal CO₂ concentration. However, recent studies have suggested that
80 separate modification of photosynthetic rate and stomatal conductance by cumulative ozone uptake in the
81 Community Land Model (CLM) leads to better representation of plant responses to ozone exposure
82 (Lombardozzi et al., 2012). This decoupling of ozone effects on photosynthesis and stomata is shown to
83 decrease water use efficiency of affected plants, but leads to an overall smaller impact of ozone on transpiration
84 and GPP than previously predicted.

85 Many climate-chemistry-biosphere modeling studies performed to date have demonstrated the
86 importance of the coevolution of climate, land cover and terrestrial ecosystems in air quality simulations and
87 predictions (Wu et al., 2012; Tai et al., 2013; Pacifico et al., 2015), but they have not taken into account the
88 potentially strong feedbacks arising from ozone damage on vegetation. For instance, ozone exposure can reduce
89 stomatal conductance and thus transpiration rate, which may modify the partition between latent and sensible
90 heat fluxes and lead to a cascade of meteorological changes: lower humidity that reduces the chemical loss rate
91 of ozone; a thicker boundary layer that dilutes all pollutants, but may enhance entrainment, which either
92 increases or decreases surface ozone depending on the vertical ozone profile (Super et al., 2015); and higher
93 temperature that enhances ozone mainly through increased biogenic emissions and higher abundance of NO_x
94 (Jacob and Winner, 2009). These transpiration-mediated pathways can be characterized as biogeophysical
95 feedbacks as are commonly known in the context of climate change, but here we prefer to call them
96 hydrometeorological or simply “meteorological feedbacks” to emphasize that they are effected through ozone-
97 induced changes in the hydrometeorological variables that ultimately affect ozone. On the other hand, reduced
98 dry deposition caused by lower stomatal conductance and a possible decline in leaf area index (LAI) following
99 ozone exposure can potentially increase ozone. The short-term impact of ozone on foliage-level isoprene
100 emission is still under debate (Fares et al., 2006; Calfapietra et al., 2007), but as foliage density (e.g.,
101 represented by LAI) declines due to chronic ozone exposure (Yue et al., 2014), isoprene emission would likely
102 decrease in the long term. These pathways directly involving plant biogeochemistry and atmospheric chemistry
103 can be collectively termed “biogeochemical feedbacks”. Fig. 1 summarizes the potentially important
104 biogeochemical and meteorological feedbacks on surface ozone concentration, which are expected to have
105 ramifications for simulations and future projections of ozone air quality. Such feedbacks may further alter
106 atmospheric composition (e.g., aerosol and oxidant concentrations) and climate at large but remain poorly
107 characterized in an Earth system modeling framework.

108 In this study, we adopt and implement a semi-empirical scheme for ozone-induced vegetation damage
109 (Lombardozzi et al., 2015) into a coupled land-atmosphere model with fully interactive atmospheric chemistry
110 and biogeochemical cycles, and examine the resulting impacts on present-day simulations of tropospheric ozone
111 air quality with respect to observations. We perform sensitivity simulations to quantify the relative importance
112 of different biogeochemical and meteorological feedback pathways, elucidate the larger sources of uncertainties,
113 and make specific suggestions regarding Earth system model development.

114 **2 Methods**

115 **2.1 Model description**

116 This study investigates the impacts of ozone-vegetation coupling on ozone concentrations using the
117 Community Earth System Model (CESM), which includes several different model components representing the
118

119 atmosphere, land, ocean, and sea ice to be run independently or in various coupled configurations (Oleson et al.,
 120 2010; Lamarque et al., 2012; Neale et al., 2013). We employ CESM version 1.2.2 with fully interactive
 121 atmosphere and land components, but with prescribed ocean and sea ice consistent with the scenarios of
 122 concern. For the atmosphere component, we use the Community Atmosphere Model version 4 (CAM4) (Neale
 123 et al., 2013) fully coupled with an atmospheric chemistry scheme (i.e., CAM-Chem) that contains full
 124 tropospheric O₃-NO_x-CO-VOC-aerosol chemistry based on the MOZART-4 chemical transport model (CTM)
 125 (Emmons et al., 2010; Lamarque et al., 2012). The version of CAM-Chem simulates the concentrations of 56
 126 atmospheric chemical species at a horizontal resolution of 1.9°×2.5° latitude-longitude and 26 vertical layers for
 127 the atmosphere up to around 40 km.

128 For the land component, we use the Community Land Model version 4 (CLM4) (Oleson et al., 2010)
 129 with active carbon-nitrogen biogeochemistry (CLM4CN), which contains prognostic treatment of terrestrial
 130 carbon and nitrogen cycles (Lawrence et al., 2011). In CLM4, the Model of Emissions of Gases and Aerosols
 131 from Nature (MEGAN) version 2.1 is used to compute biogenic emissions online as functions of changing LAI,
 132 vegetation temperature, soil moisture and other environmental conditions (Guenther et al., 2012). For dry
 133 deposition of gases and aerosols we use the resistance-in-series scheme in CLM4 as described in Lamarque et
 134 al. (2012) with a further update of optimized coupling of stomatal resistance to LAI (Val Martin et al., 2014).
 135 Evapotranspiration is calculated based on the Monin-Obukhov similarity theory and the diffusive flux-resistance
 136 model with dependence on vegetation, ground and surface temperature, specific humidity, and an ensemble of
 137 resistances that are functions of meteorological and land surface conditions (Oleson et al., 2010; Lawrence et al.,
 138 2011; Bonan et al., 2011). Evapotranspiration is partitioned into transpiration, ground evaporation and canopy
 139 evaporation, with updates from Lawrence et al. (2011), and is linked to photosynthesis via the computation of
 140 stomatal resistance, as described below.

141

142 **2.2 Photosynthesis- stomatal conductance model and ozone damage parameterization**

143 The Farquhar/Ball-Berry model is used in CLM4CN to compute leaf-level photosynthetic rate and
 144 stomatal conductance under different environmental conditions (Farquhar et al., 1980; Ball et al., 1987). Leaf
 145 photosynthetic rate, A ($\mu\text{mol CO}_2 \text{ m}^{-2} \text{ s}^{-1}$), is calculated as

$$146 \quad A = \min(W_c, W_j, W_e) \quad (1)$$

147 where W_c is the Ribulose-1,5-bisphosphate carboxylase (RuBisCO)-limited rate of carboxylation, W_j is the light-
 148 limited rate, and W_e is the export-limited rate. Photosynthesis and stomatal conductance (g_s) are related by

$$149 \quad g_s = \frac{1}{r_s} = m \frac{A e_s}{c_s e_i} P_{\text{atm}} + b \quad (2)$$

150 where g_s is the leaf stomatal conductance; r_s is the leaf stomatal resistance ($\text{s m}^2 \mu\text{mol}^{-1}$); m is the slope of the
 151 conductance-photosynthesis relationship with values ranging from 5 to 9; c_s is the CO₂ partial pressure at leaf
 152 surface (Pa); e_s is the vapor pressure at leaf surface (Pa); e_i is the saturation vapor pressure inside the leaf (Pa);
 153 P_{atm} is the atmospheric pressure (Pa); and b is the minimum stomatal conductance when $A = 0$, and is set to give
 154 a maximum stomatal resistance of 20000 s m^{-1} in CLM4 (Oleson et al., 2010).

155 Parameterization for the impact of ozone exposure on photosynthesis and stomatal conductance follows
 156 the work of Lombardozzi et al., (2015), who tested the sensitivity of global ecosystem productivity and
 157 hydrometeorology to ozone damage on vegetation using satellite phenology (i.e., prescribed LAI, canopy height,
 158 etc.) and present-day ozone concentrations. The scheme uses two sets of ozone impact factors, one for

159 modifying photosynthetic rate and another for stomatal conductance independently. These factors account for
 160 different plant groups, and are calculated based on the cumulative uptake of ozone (CUO) under different levels
 161 of chronic ozone exposure (Lombardozzi et al., 2013). CUO (mmol m^{-2}) integrates ozone flux into leaves over
 162 the growing season as

$$163 \quad \text{CUO} = 10^{-6} \sum \frac{[\text{O}_3]}{k_{\text{O}_3} r_s + r_a} \Delta t \quad (3)$$

164 where $[\text{O}_3]$ is the instantaneous surface ozone concentration (nmol m^{-3}) computed from CAM-Chem at a given
 165 model time step Δt ($\Delta t = 1800$ s here); $k_{\text{O}_3} = 1.67$ is the ratio of leaf resistance to ozone to leaf resistance to
 166 water, r_s is the stomatal resistance (s m^{-1}), and r_a is the boundary layer and aerodynamic resistance between leaf
 167 surface and reference level (s m^{-1}) (Sitch et al., 2007). Ozone uptake is only cumulated over time steps during
 168 the growing season when vegetation is most vulnerable to air pollution episodes; growing season is defined as
 169 the period in which total leaf area index (TLAI) > 0.5 (Lombardozzi et al., 2012). Ozone uptake only cumulates
 170 when the ozone flux is above an instantaneous critical threshold, $0.8 \text{ nmol O}_3 \text{ m}^{-2} \text{ s}^{-1}$, to account for ozone
 171 detoxification by vegetation at lower ozone levels (Lombardozzi et al., 2015). Three different plant groups are
 172 accounted for: evergreen, deciduous, and crops/grasses. We also include a leaf-turnover ozone decay rate for
 173 evergreen plants so that accumulated ozone damage does not accrue beyond the average foliar lifetime. The
 174 ozone impact factors have empirical linear relationships with CUO such that

$$175 \quad F_{p\text{O}_3} = a_p \times \text{CUO} + b_p \quad (4)$$

$$176 \quad F_{c\text{O}_3} = a_c \times \text{CUO} + b_c \quad (5)$$

177 where $F_{p\text{O}_3}$ is the ozone damage factor multiplied to the photosynthesis rate (A), and a_p and b_p are slope and
 178 intercept from empirical and experimental studies (listed in Table 1); $F_{c\text{O}_3}$ is the ozone damage factor multiplied
 179 with stomatal conductance (g_s), and a_c and b_c are the corresponding slope and intercept (Table 1). The ozone
 180 damage is applied to the optimal photosynthesis and stomatal conductance values, which are calculated
 181 iteratively first without ozone damage, to allow the damage to be applied independently.

182

183 **2.3 Model experiments**

184 Incorporating the ozone-vegetation parameterization above into CLM4CN and coupling it with CAM-
 185 Chem, we allow, for the first time, ecosystem structure (e.g., in terms of LAI and canopy height) to evolve in
 186 response to ozone exposure but at the same time allow ozone concentration to evolve in response to such
 187 ecosystem changes. Therefore, previously discussed feedbacks are mostly included. We conduct four sets of
 188 fully coupled land-atmosphere simulations: 1) a control case without ozone damage on vegetation ([CTR]); 2)
 189 simulation with both photosynthetic rate and stomatal conductance modified by ozone impact factors
 190 (independently) ([PHT+COND]), following the approach of Lombardozzi et al (2015); 3) simulation where we
 191 apply the ozone impact factor to photosynthetic rate only ([PHT]), but stomatal conductance is calculated using
 192 the intact, optimal photosynthetic rate; and 4) simulation where we apply the ozone impact factor to stomatal
 193 conductance only ([COND]), but photosynthetic rate is calculated using the intact stomatal conductance.

194 Simulations [PHT] and [COND], when compared with [PHT+COND], allow us to quantify the relative
195 contribution from each pathway. To determine the relative contribution of those pathways involving biogenic
196 emissions toward the overall ozone-vegetation feedback, we conduct an additional set of sensitivity simulations
197 with prescribed isoprene emission and MEGAN turned off: a control case with no MEGAN (CTR_nM), and a
198 simulation with modified photosynthesis and stomatal conductance but with no MEGAN ([PHT+COND_nM]).
199 To determine the relative contribution of pathways involving dry deposition vs. transpiration, we compare
200 simulated results with that of Val Martin et al. (2014) who have used the similar CAM-Chem-CLM framework
201 but without ozone-vegetation coupling to test the sensitivity of ozone to perturbations in dry deposition velocity.

202 All simulations are conducted for 20 years using year 2000 initial conditions and the corresponding
203 land cover data (e.g., land cover and land use types, satellite LAI, etc.). The first five years of outputs are treated
204 as spin-up and thus discarded in the analysis. We observe that the annual averages of key aboveground
205 ecosystem parameters such as LAI and ozone concentration come into a relatively steady state after 5 years. We
206 focus on changes in the 15-year northern summertime (JJA) averages for most of the variables in the rest of this
207 paper because this is the period when the growing season of the majority of global vegetation overlaps most
208 significantly with high-ozone season especially in the northern midlatitudes.

209

210 **3 Simulated ozone with and without ozone-vegetation coupling**

211 Figure 2 shows the 15-year mean summertime surface ozone concentration from the [PHT+COND]
212 simulation. The corresponding cumulative uptake of ozone (CUO) used to affect vegetation is shown in
213 supplemental Fig. S1. Simulated ozone is generally higher in the northern midlatitudes than elsewhere, and is
214 the highest over the Mediterranean where solar radiation is particularly strong. CUO also has high values in
215 Europe, but the overall distribution does not exactly follow that of surface ozone concentration because CUO
216 also depends on the length of the growing season and stomatal conductance. CUO ranges between 20-70 mmol
217 m⁻² over regions with both high summertime ozone and high productivity. The simulated CUO is comparable in
218 both magnitude and spatial distribution with Lombardozzi et al., (2015), who used prescribed meteorology,
219 ozone and vegetation phenology with no active carbon-nitrogen cycle or atmospheric coupling, as opposed to
220 this study. This suggests that online ozone-vegetation coupling, which can modify ozone concentration
221 substantially depending on the region, leads to a similar pattern of ozone uptake by vegetation to the case using
222 prescribed ozone due to the compensation between higher (lower) concentration and higher (lower) stomatal
223 resistance, as reflected in Eq. (3). During the growing season, CUO is used to calculate the ozone impact factors
224 that modify photosynthetic rate and stomatal conductance according to Eq. (4) and (5) and parameter values
225 listed in Table 1.

226 Figure 3 shows the differences in surface ozone concentration in different simulations from the control
227 case (corresponding relative changes shown in supplemental Fig. S2). Implementing ozone-vegetation coupling
228 that includes simultaneous modification of photosynthetic rate and stomatal conductance by ozone exposure (the
229 [PHT+COND] case) increases mean surface ozone globally, and significant increases by up to 4-6 ppbv are
230 found over China, North America and Europe (Fig. 3a). Ozone exposure is thus found to constitute a positive
231 feedback loop via vegetation that ultimately enhances surface ozone levels when ozone-vegetation coupling is
232 accounted for.

233 The simulated increases in ozone levels due to ozone-vegetation coupling are significant when
234 compared with the possible impacts of 2000-2050 climate and land cover changes on surface ozone, which are
235 in the range of +1-10 ppbv (Jacob & Winner, 2009; Tai et al., 2013; Val Martin et al., 2015). [This coupling](#)
236 [effect is smaller than the potential ozone changes driven by anthropogenic emissions \(up to +30 ppbv\), but it](#)
237 [more likely reflects compensation among various pathways \(e.g., Ganzeveld et al., 2010\).](#) These simulated
238 increases, however, slightly worsen the performance of CAM-Chem in reproducing ozone concentrations
239 against observations as seen in Fig. 4, which shows the model-observation comparison for the control case
240 (standard CAM-Chem-CLM with dry deposition improvement of Val Martin et al. (2014)) and the
241 [PHT+COND] case. The high-biases in CESM-simulated summertime surface ozone concentrations in North
242 America and Europe are a commonly acknowledged issue with CAM-Chem (Lamarque et al., 2012) and other
243 global and regional models (Lapina et al., 2014; Parrish et al., 2014). Uncertain emissions, coarse resolution
244 (Lamarque et al., 2012), misrepresentation of dry deposition process and overestimation of stomatal resistance
245 (Val Martin et al., 2014) are all likely factors contributing to these high biases. Inclusion of ozone-vegetation
246 coupling in the model further increases the normalized mean biases of the modeled results against three sets of
247 observational data: Clean Air Status and Trends Network (CASTNET) (1999-2001), Air Quality System (AQS)
248 (1999-2001), and European Monitoring and Evaluation Programme (EMEP) (1999-2001), from 18% to 22%,
249 31% to 35%, 14% to 22%, respectively. Although there remains considerable uncertainty in the
250 parameterization of ozone-vegetation coupling and in ozone simulations by Earth system models, we show that
251 including ozone damage in a coupled climate-chemistry-biosphere framework can have a potentially significant
252 impact on surface ozone simulations.

253

254 **4 Attribution to different biogeochemical and meteorological feedback pathways**

255 Figures 3(b) and 3(c) show the differences in ozone for the cases where ozone damages stomatal
256 conductance alone and photosynthesis alone, respectively, noting that each of them is calculated using the
257 undamaged, intact values of the other variable. Comparison of Fig. 3(a) with (b)-(c) shows that the modification
258 of stomatal conductance by ozone uptake contributes more dominantly to the overall effect of ozone-vegetation
259 coupling (Fig. 3a). This suggests that, among the various feedback pathways that may influence surface ozone
260 (Fig. 1), those triggered by changes in stomatal conductance are generally more important than those associated
261 with photosynthesis or the associated changes in ecosystem production and structure including LAI, at least in
262 the modeling framework of this study. This is also supported by sensitivity simulations performed under the
263 same modeling framework but without ozone damage, in which a 50% of increase in LAI decreases
264 summertime surface ozone by on average 3 ppb, which is relatively small in comparison with the changes
265 following optimization of stomatal resistance (Val Martin et al., 2014). Indeed, the effect of modifying stomatal
266 conductance alone ([COND]; Fig. 3b) is slightly larger than the case of [PHT+COND] (Fig. 3a), where the
267 additional effect of modifying photosynthesis together with stomatal conductance would slightly offset the
268 overall positive feedback on ozone. It is noteworthy that this additional effect is, however, not consistent with
269 the effect of modifying photosynthesis alone ([PHT]; Fig. 3c), reflecting nonlinear interactions between
270 photosynthesis and stomatal conductance.

271 Figure 5 shows the differences in dry deposition velocity, transpiration rate and biogenic isoprene
272 emission between the [PHT+COND] and [CTR] simulations (relative changes shown in supplemental Fig. S3).

273 Over China, Europe and North America, ozone dry deposition velocity is lower (by up to ~20%) in
274 [PHT+COND]. In these same regions but especially in the eastern US, southern Europe and southern China,
275 isoprene emission is significantly higher (by up to ~50%). In addition, in similar regions but especially in
276 central North America, the transpiration rate is reduced by ozone exposure (by up to ~20%), which would
277 reduce boundary-layer humidity, increase surface temperature, enhance dry convection and thicken the
278 boundary layer. In view of Fig. 1, all of these pathways may add to or offset each other, leading to the overall
279 ozone changes seen in Fig. 3(a). The sensitivity simulations and comparison with Val Martin et al. (2014), which
280 examined the sensitivity of simulated ozone to differences in dry deposition schemes under essentially the same
281 modeling framework, allow us to quantify more precisely which of these pathways are more important as we
282 discuss next.

283 Figure 6(a) shows the changes in surface ozone in the [PHT+COND_nM] minus CTR_nM simulations,
284 where we use prescribed biogenic emissions from the original control case (CTR) to drive ozone chemistry so
285 that we essentially shut down any feedback pathways involving biogenic emissions. A comparison between Fig.
286 6(a) and Fig. 3(a) shows that the changes in [biogenic VOC emissions](#) account for ~0-60% of the ozone increases
287 over Europe, North America and China, while dry deposition and/or transpiration-driven meteorological
288 changes (excluding the temperature effect on isoprene emission) account for remaining ~40-100%. We further
289 show in Fig. 6(b) the theoretical changes in surface ozone by multiplying the dry deposition changes in Fig. 5(a)
290 by the change in ozone concentration per unit change in dry deposition velocity from the study of Val Martin et
291 al. (2014), [which provided an approximate sensitivity of simulated ozone to perturbed dry deposition velocity](#)
292 [only to separate this impact from that due to hydrometeorological changes associated with changing stomatal](#)
293 [conductance](#), e.g., changes in mixing depth. We find that the ozone changes in Fig. 6(a) and Fig. 6(b) are similar
294 in magnitude, suggesting that globally most of the non-isoprene-driven differences in ozone is driven by dry
295 deposition. Notable exceptions include the US Midwest and southeastern Europe, where higher mixing depth
296 following reduced transpiration might have partly offset the ozone positive feedback, [whereas in western](#)
297 [Europe the lower chemical loss rate following reduced transpired water might have further enhanced the](#)
298 [positive feedback](#).

299 The simulated general reduction in dry deposition velocity and transpiration rate (Fig. 5a and 5b) is
300 mostly due to increased stomatal resistance (Fig. 7a), i.e., reduced stomatal conductance, a direct response to
301 cumulative uptake of ozone. The reduced [dry deposition velocity](#) represents a positive biogeochemical feedback
302 on ozone (orange arrows in Fig. 1). The simulated increase in biogenic isoprene emission (Fig. 5c) is found to
303 be mostly driven by higher surface (thus vegetation) temperature (Fig. 7b) that results from lower transpiration
304 rate and latent heat flux (Fig. 7c). Therefore, this feedback loop involving biogenic emissions is indeed an
305 indirect, meteorological feedback that is also initiated by stomatal and transpiration changes (purple arrows in
306 Fig. 1). Relative changes in variables shown in Fig. 7 are included in supplemental Fig. S4.

307 By including immediate ozone-vegetation coupling, we find a larger decline in transpiration rate (6.4%
308 globally) than in the offline, uncoupled land model results (2.0-2.4%) estimated by Lombardozzi et al. (2015).
309 On the other hand, although reduced photosynthesis and the resulting long-term changes in GPP and LAI (Fig.
310 7d-e) play a smaller role than reduced stomatal conductance in shaping simulated ozone (Fig. 3b-c), the impacts
311 are not negligible (up to 3 ppb), especially as these changes are also nonlinearly coupled to stomatal changes.
312 Photosynthetic rate decreases by up to 20% directly due to the ozone effect (Fig. 7f), which is quite similar both

313 in magnitude and spatial pattern to the results of Lombardozzi et al. (2015), but the corresponding GPP and LAI
314 changes are relatively small (~5% over regions concerned, except for Southeast Asia, where the highest ozone-
315 induced LAI reduction is simulated and leads to isoprene emission decrease despite higher surface temperature).
316 Grid-level GPP and LAI in certain areas increase despite reduced leaf-level photosynthetic rate, likely reflecting
317 more carbon allocation to leaves to compensate the reduced photosynthetic rate and relaxation of resource
318 limitation as nutrients and water become less limiting upon lower photosynthetic and evaporative demands, as
319 well as favorable hydrometeorological changes following ozone exposure (enhanced soil moisture and
320 precipitation as shown in Fig. S5). These LAI increases induced by ozone are not represented in Fig. 1 because
321 they more likely reflect the fully coupled effect of changing hydrometeorology, instead of the direct effect of
322 ozone on LAI as is typically observed in experimental studies (Ainsworth et al., 2012).

323

324 5 Conclusions and discussion

325 Tropospheric ozone is one the most hazardous air pollutants due to its harmful effects on human health
326 and damage to forest and agricultural productivity. Stomatal uptake of ozone by leaves reduces both
327 photosynthetic rate and stomatal conductance. These vegetation changes can induce a cascade of
328 biogeochemical and biogeophysical (or meteorological) effects (Fig. 1) that ultimately modulate climate, carbon
329 cycle and also feedback onto ozone air quality itself. The direct, biogeochemical feedback pathways include
330 reduced ozone dry deposition and biogenic VOC emissions. The indirect, meteorological feedback pathways are
331 facilitated by transpiration-driven changes in the meteorological environment that influence ozone formation
332 and removal. A few land surface modeling studies have estimated the direct effects of ozone on ecosystem
333 production and land-atmosphere water exchange (Yue and Unger, 2014; Lombardozzi et al., 2015), and
334 predicted a possible positive radiative forcing from the ozone-induced decline in the land-carbon sink (Sitch et
335 al., 2007).

336 In this study, we implement a semi-empirical parameterization of ozone damage on vegetation
337 (Lombardozzi et al., 2015) into the CESM (CAM4-Chem-CLM4CN) modeling framework to enable online
338 ozone-vegetation coupling so that vegetation variables can evolve in response to ozone exposure, and at the
339 same time simulated ozone concentration can respond to ecosystem changes. Our scheme modifies leaf-level
340 photosynthesis and stomatal conductance separately via the ozone impact factors, which are assumed to have
341 empirical linear relationships with cumulative uptake of ozone and account for different plant groups.
342 Sensitivity simulations are conducted to determine the relative importance of different feedback pathways.

343 With ozone-vegetation coupling, surface ozone is simulated to be higher by up to 4-6 ppbv over
344 Europe, North America and China. This coupling effect is significant in view of the 2000-2050 effects of
345 climate and land cover changes on surface ozone (+1-10 ppbv) as found in previous work (Jacob and Winner,
346 2009; Ganzeveld et al., 2010; Tai et al., 2013), and should be considered in future air quality projection studies.
347 Reduced dry deposition velocity following the modification contributes to ~40-100% and enhanced biogenic
348 isoprene emission contributes to ~0-60% of the higher ozone concentrations. The dry deposition-driven ozone
349 increases (by up to 4 ppbv) arise mostly from reduced stomatal conductance, and are consistent with the
350 sensitivity of ozone to perturbations in dry deposition velocity found by Val Martin et al. (2014). This pathway
351 constitutes a significant positive biogeochemical feedback on surface ozone. The other major feedback
352 associated with enhanced isoprene emission is mostly driven by higher vegetation temperature that results from

353 lower transpiration rate. This pathway constitutes an indirect, positive meteorological feedback on surface
354 ozone. Depending on the region, transpiration-driven meteorological changes such as lower humidity and
355 deeper mixing depth may also influence surface ozone. Transpiration rate is simulated to decrease by 6.4%
356 globally, which is a larger change compared with the decrease estimated by Lombardozzi et al. (2015), who
357 used prescribed instead of synchronously simulated atmospheric forcings. This also suggests an augmented
358 effect on transpiration due to changes in carbon allocation and foliage density arising from ozone-vegetation
359 coupling.

360 Modification of photosynthesis and further long-term changes in ecosystem productivity and structure,
361 including LAI changes, are found to play a smaller role in contributing to the ozone-vegetation feedbacks than
362 direct stomatal changes, but are not insignificant (up to +3 ppbv). The simulated changes in LAI (less than 5%)
363 in this study are similar in magnitude to that by Yue et al. (2015), who included an active carbon cycle though
364 using Yale Interactive terrestrial Biosphere (YIBs) model with a different ozone-vegetation parameterization.
365 However, prognostic treatment of the carbon cycle and LAI calculation in CLM4CN are still known to be
366 problematic, with large uncertainties and biases in the estimation of global carbon fluxes (Sun et al., 2012),
367 arising from incomplete model parameterization and from uncertainty in photosynthetic parameters (Bonan et
368 al., 2011). It is not surprising that changes in GPP as simulated here do not replicate the results of Lombardozzi
369 et al. (2015), in which vegetation phenology is prescribed and the carbon and nitrogen cycles are not active
370 (CLM4.5SP). Implementing ozone damage on vegetation in a model with more sophisticated and realistic
371 representation of prognostic carbon-nitrogen cycle is highly warranted, so that the possible effects of ozone-
372 induced long-term ecosystem changes can be examined more fully.

373 Large variability in the responses of different plants to ozone leads to considerable uncertainties in any
374 global-scale studies (Lombardozzi et al., 2013). Such large variability in plant responses across different studies,
375 in some cases, weakens the correlation between phytotoxic responses and CUO. Such correlation is usually
376 more evident in individual studies, and in the parametrization schemes based on them (Sitch et al., 2007; Yue et
377 al., 2014). The parameterization developed by Lombardozzi et al. (2013), based on the most comprehensive
378 database available for photosynthetic and stomatal responses to CUO to date, is deemed more appropriate for
379 the global scale of this study and the plant functional types represented in the model, despite the weaker
380 correlation between plant responses and CUO as shown by the compilation of data across studies. The damage
381 is applied after CUO reaches a certain threshold, so the calculation of CUO is still crucial to the application of
382 the damage functions. The model results could possibly be improved with more detailed plant-type-specific
383 ozone damage parameterization, including better estimates of plant vulnerability to ozone that will help refine
384 the ozone uptake thresholds (Lombardozzi et al., 2015). An important caveat of this study is the consideration of
385 only three plant groups to generalize the responses of global vegetation to ozone exposure because data are
386 largely unavailable for other plant groups.

387 Another potential caveat is the uncertainty and lack of cross-validation in hydrometeorological
388 simulations with respect to the ozone phytotoxicity scheme we newly implement, as we only focus on
389 vegetation and atmospheric chemical changes in this study. Although most simulated vegetation variables are
390 consistent with previous work, the changes in simulated vegetation temperature from ozone-vegetation coupling
391 are not small (by up to +2°C) (Fig. 7b) and they result in quite substantial changes in isoprene emission,
392 suggesting the need for further tuning of hydrometeorological processes in the model. Also, MEGAN does not

393 consider the direct, immediate biochemical connection between photosynthesis and biogenic emissions, by
394 which ozone damage on photosynthesis may directly reduce isoprene emission and partially offset the
395 significant temperature-induced increase in isoprene emission as shown in Fig. 5c (Tiwari et al., 2015). Whereas
396 the various environmental activity factors used in MEGAN to adjust baseline emissions may have implicitly
397 encapsulated the biochemical connection with photosynthesis, further incorporating such connection into ozone-
398 vegetation modeling warrants more in-depth investigation. In general, we have the highest confidence in the
399 quantification of the biogeochemical pathway via stomata-driven deposition changes, which is straightforward
400 and accounts for the majority of the ozone-vegetation feedbacks. On the other hand, the hydrometeorological
401 feedbacks introduce strong nonlinearity in the interactions between atmospheric chemistry, soil moisture and
402 vegetation that is more difficult to isolate. Parameterizing the ozone-vegetation coupling in a standalone
403 chemical transport model with prescribed meteorology could be particularly helpful to more confidently
404 separate between the effects of biogeochemical vs. meteorological feedbacks. This knowledge will be important
405 in projecting the impacts of future climate and land cover changes on ozone air quality and climate feedbacks in
406 the coming decades.

407

408 **Acknowledgment**

409 This work was supported by the Early Career Scheme (Project Number: 24300614) of the Research
410 Grants Council of Hong Kong, and the associated Direct Grant for Research (Project ID: 4441337, 3132767)
411 from The Chinese University of Hong Kong (CUHK), given to the principal investigator, Amos P. K. Tai. We
412 also thank the Information Technology Services Centre (ITSC) at CUHK for their devotion in providing the
413 necessary computational services for this work.

414

415 **References**

- 416 Ainsworth, E. A., Yendrek, C. R., Sitch, S., Collins, W. J., and Emberson, L. D.: The Effects of Tropospheric
417 Ozone on Net Primary Productivity and Implications for Climate Change, *Annu Rev Plant Biol*, 63, 637-661,
418 doi: 10.1146/annurev-arplant-042110-103829, 2012.
- 419 Anenberg, S. C., Horowitz, L. W., Tong, D. Q., and West, J. J.: An Estimate of the Global Burden of
420 Anthropogenic Ozone and Fine Particulate Matter on Premature Human Mortality Using Atmospheric
421 Modeling, *Environ Health Persp*, 118, 1189-1195, doi:10.1289/ehp.0901220, 2010.
- 422 Ashmore, M. R.: Assessing the future global impacts of ozone on vegetation, *Plant Cell Environ*, 28, 949-964,
423 doi:10.1111/J.1365-3040.2005.01341.X, 2005.
- 424 Ball, J. T., Woodrow, I. E., and Berry, J. A.: A model predicting stomatal conductance and its contribution to the
425 control of photosynthesis under different environmental conditions, *Prog. Photosynthesis*, 221-224, 1987.
- 426 Bernacchi, C. J., Leakey, A. D. B., Kimball, B. A., and Ort, D. R.: Growth of soybean at future tropospheric
427 ozone concentrations decreases canopy evapotranspiration and soil water depletion, *Environ Pollut*, 159, 1464-
428 1472, doi:10.1016/j.envpol.2011.03.011, 2011.
- 429 Bonan, G. B.: Forests and climate change: Forcings, feedbacks, and the climate benefits of forests, *Science*, 320,
430 1444-1449, doi:10.1126/science.1155121, 2008.
- 431 Bonan, G. B., Lawrence, P. J., Oleson, K. W., Levis, S., Jung, M., Reichstein, M., Lawrence, D. M., and
432 Swenson, S. C.: Improving canopy processes in the Community Land Model version 4 (CLM4) using global

433 flux fields empirically inferred from FLUXNET data, *J Geophys Res-Biogeosci*, 116, G02014,
434 doi:10.1029/2010jg001593, 2011.

435 Calfapietra, C., Wiberley, A. E., Falbel, T. G., Linskey, A. R., Mugnoz, G. S., Karnosky, D. F., Loreto, F., and
436 Sharkey, T. D.: Isoprene synthase expression and protein levels are reduced under elevated O₃ but not under
437 elevated CO₂ (FACE) in field-grown aspen trees, *Plant Cell Environ*, 30, 654-661, doi:10.1111/j.1365-
438 3040.2007.01646.x, 2007.

439 Collins, W. J., Sitch, S., and Boucher, O.: How vegetation impacts affect climate metrics for ozone precursors, *J*
440 *Geophys Res-Atmos*, 115, D23308, doi:10.1029/2010jd014187, 2010.

441 Emmons, L. K., Walters, S., Hess, P. G., Lamarque, J. F., Pfister, G. G., Fillmore, D., Granier, C., Guenther, A.,
442 Kinnison, D., Laepple, T., Orlando, J., Tie, X., Tyndall, G., Wiedinmyer, C., Baughcum, S. L., and Kloster, S.:
443 Description and evaluation of the Model for Ozone and Related chemical Tracers, version 4 (MOZART-4),
444 *Geosci Model Dev*, 3, 43-67, 2010.

445 Fares, S., Barta, C., Brilli, F., Centritto, M., Ederli, L., Ferranti, F., Pasqualini, S., Reale, L., Tricoli, D., and
446 Loreto, F.: Impact of high ozone on isoprene emission, photosynthesis and histology of developing *Populus alba*
447 leaves directly or indirectly exposed to the pollutant, *Physiol Plantarum*, 128, 456-465, doi: 10.1111/j.1399-
448 3054.2006.00750.x, 2006.

449 Farquhar, G. D., Caemmerer, S. V., and Berry, J. A.: A Biochemical-Model of Photosynthetic Co₂ Assimilation
450 in Leaves of C-3 Species, *Planta*, 149, 78-90, doi:10.1007/Bf00386231, 1980.

451 Fiore, A. M., Levy, H., and Jaffe, D. A.: North American isoprene influence on intercontinental ozone pollution,
452 *Atmos Chem Phys*, 11, 1697-1710, doi:10.5194/acp-11-1697-2011, 2011.

453 [Ganzeveld, L., Bouwman, L., Stehfest, E., van Vuuren, D. P., Eickhout, B., and Lelieveld, J.: Impact of future
454 land use and land cover changes on atmospheric chemistry-climate interactions, *J Geophys Res*, 115, D23301,
455 doi:10.1029/2010JD014041, 2010.](#)

456 Gauss, M., Myhre, G., Pitari, G., Prather, M. J., Isaksen, I. S. A., Bernsten, T. K., Brasseur, G. P., Dentener, F. J.,
457 Derwent, R. G., Hauglustaine, D. A., Horowitz, L. W., Jacob, D. J., Johnson, M., Law, K. S., Mickley, L. J.,
458 Muller, J. F., Plantevin, P. H., Pyle, J. A., Rogers, H. L., Stevenson, D. S., Sundet, J. K., van Weele, M., and
459 Wild, O.: Radiative forcing in the 21st century due to ozone changes in the troposphere and the lower
460 stratosphere, *J Geophys Res-Atmos*, 108, 4292, doi:10.1029/2002jd002624, 2003.

461 Guenther, A. B., Jiang, X., Heald, C. L., Sakulyanontvittaya, T., Duhl, T., Emmons, L. K., and Wang, X.: The
462 Model of Emissions of Gases and Aerosols from Nature version 2.1 (MEGAN2.1): an extended and updated
463 framework for modeling biogenic emissions, *Geosci Model Dev*, 5, 1471-1492, doi:10.5194/gmd-5-1471-2012,
464 2012.

465 Herbinger, K., Then, C., Haberer, K., Alexou, M., Low, M., Remele, K., Rennenberg, H., Matyssek, R., Grill,
466 D., Wieser, G., and Tausz, M.: Gas exchange and antioxidative compounds in young beech trees under free-air
467 ozone exposure and comparisons to adult trees, *Plant Biol*, 9, 288-297, doi:10.1055/s-2006-924660, 2007.

468 Jacob, D. J., and Winner, D. A.: Effect of climate change on air quality, *Atmos Environ*, 43(1), 51-63,
469 doi:10.1016/j.atmosenv.2008.09.051, 2009.

470 Karnosky, D. F., Skelly, J. M., Percy, K. E., and Chappelka, A. H.: Perspectives regarding 50 years of research
471 on effects of tropospheric ozone air pollution on US forests, *Environ Pollut*, 147, 489-506,
472 doi:10.1016/j.envpol.2006.08.043, 2007.

473 Kroeger, T., Escobedo, F. J., Hernandez, J. L., Varela, S., Delphin, S., Fisher, J. R., and Waldron, J.:

474 Reforestation as a novel abatement and compliance measure for ground-level ozone, *P Natl A Sci*, 111(40),

475 E4204-E4213, doi:10.1073/pnas.1409785111, 2014.

476 Lamarque, J. F., Emmons, L. K., Hess, P. G., Kinnison, D. E., Tilmes, S., Vitt, F., Heald, C. L., Holland, E. A.,

477 Lauritzen, P. H., Neu, J., Orlando, J. J., Rasch, P. J., and Tyndall, G. K.: CAM-chem: description and evaluation

478 of interactive atmospheric chemistry in the Community Earth System Model, *Geosci Model Dev*, 5, 369-411,

479 doi:10.5194/gmd-5-369-2012, 2012.

480 Lapina, K., Henze, D. K., Milford, J. B., Huang, M., Lin, M., Fiore, A. M., Carmichael, G., Pfister, G. G., and

481 Bowman, K.: Assessment of source contributions to seasonal vegetative exposure to ozone in the US, *J Geophys*

482 *Res-Atmos*, 119(1), 324-340, doi: 10.1002/2013JD020905, 2014.

483 Lawrence, D. M., Oleson, K. W., Flanner, M. G., Thornton, P. E., Swenson, S. C., Lawrence, P. J., Zeng, X. B.,

484 Yang, Z. L., Levis, S., Sakaguchi, K., Bonan, G. B., and Slater, A. G.: Parameterization Improvements and

485 Functional and Structural Advances in Version 4 of the Community Land Model, *J Adv Model Earth Sy*, 3,

486 M03001, doi:10.1029/2011ms000045, 2011.

487 Lombardozzi, D., Sparks, J. P., Bonan, G., and Levis, S.: Ozone exposure causes a decoupling of conductance

488 and photosynthesis: implications for the Ball-Berry stomatal conductance model, *Oecologia*, 169, 651-659,

489 doi:10.1007/s00442-011-2242-3, 2012.

490 Lombardozzi, D., Sparks, J. P., and Bonan, G.: Integrating O₃ influences on terrestrial processes: photosynthetic

491 and stomatal response data available for regional and global modeling, *Biogeosciences*, 10, 6815-6831,

492 doi:10.5194/bg-10-6815-2013, 2013.

493 Lombardozzi, D., Levis, S., Bonan, G., Hess, P. G., and Sparks, J. P.: The Influence of Chronic Ozone Exposure

494 on Global Carbon and Water Cycles, *J Climate*, 28, 292-305, doi:10.1175/JCLI-D-14-00223.1, 2015.

495 Marengo, A., Gouget, H., Nedelec, P., Pages, J. P., and Karcher, F.: Evidence of a Long-Term Increase in

496 Tropospheric Ozone from Pic Du Midi Data Series - Consequences - Positive Radiative Forcing, *J Geophys*

497 *Res-Atmos*, 99, 16617-16632, doi:10.1029/94jd00021, 1994.

498 Neale, R. B., Richter, J., Park, S., Lauritzen, P. H., Vavrus, S. J., Rasch, P. J., and Zhang, M. H.: The Mean

499 Climate of the Community Atmosphere Model (CAM4) in Forced SST and Fully Coupled Experiments, *J*

500 *Climate*, 26, 5150-5168, doi:10.1175/JCLI-D-12-00236.1, 2013.

501 Oleson, K. W., Lawrence, D. M., Gordon, B., Flanner, M. G., Kluzek, E., Peter, J., Levis, S., Swenson, S. C.,

502 Thornton, E., and Feddema, J.: Technical description of version 4.0 of the Community Land Model (CLM),

503 2010.

504 Pacifico, F., Folberth, G. A., Sitch, S., Haywood, J. M., Rizzo, L. V., Malavelle, F. F., and Artaxo, P.: Biomass

505 burning related ozone damage on vegetation over the Amazon forest: a model sensitivity study, *Atmos Chem*

506 *Phys*, 15, 2791-2804, doi:10.5194/acp-15-2791-2015, 2015.

507 Parrish, D. D., Lamarque, J. F., Naik, V., Horowitz, L., Shindell, D. T., Staehelin, J., Derwent, R., Cooper, O. R.,

508 Tanimoto, H., Volz-Thomas, A., and Gilge, S.: Long-term changes in lower tropospheric baseline ozone

509 concentrations: Comparing chemistry-climate models and observations at northern midlatitudes, *J Geophys Res-*

510 *Atmos*, 119(9), 5719-5736, doi: 10.1002/2013JD021435, 2014.

511 Sitch, S., Cox, P. M., Collins, W. J., and Huntingford, C.: Indirect radiative forcing of climate change through

512 ozone effects on the land-carbon sink, *Nature*, 448, 791-U794, doi:10.1038/nature06059, 2007.

513 Sun, Y., Gu, L. H., and Dickinson, R. E.: A numerical issue in calculating the coupled carbon and water fluxes in
514 a climate model, *J Geophys Res-Atmos*, 117, D22103, doi:10.1029/2012jd018059, 2012.

515 [Super, I., Vilà-Guerau de Arellano, J., and Krol, M. C.: Cumulative ozone effect on canopy stomatal resistance
516 and the impact on boundary layer dynamics and CO₂ assimilation at the diurnal scale: A case study for
517 grassland in the Netherlands, *J Geophys Res-Bioge*, 120\(7\), 1348-1365, doi:10.1002/2015JG002996, 2015.](#)

518 Tai, A. P. K., Mickley, L. J., Heald, C. L., and Wu, S. L.: Effect of CO₂ inhibition on biogenic isoprene emission:
519 Implications for air quality under 2000 to 2050 changes in climate, vegetation, and land use, *Geophys Res Lett*,
520 40, 3479-3483, doi:10.1002/grl.50650, 2013.

521 Tiwari, S., Grote, R., Churkina, G., and Butlet, T.: Ozone damage, detoxification and the role of isoprenoids -
522 new impetus for integrated models, *Funct Plant Biol*, 43(4) 324-336, 2016.

523 Val Martin, M., Heald, C. L., and Arnold, S. R.: Coupling dry deposition to vegetation phenology in the
524 Community Earth System Model: Implications for the simulation of surface O₃, *Geophys Res Lett*, 41(8), 2988-
525 2996, doi:10.1002/2014GL059651, 2014.

526 Val Martin, M., Heald, C. L., Lamarque, J. F., Tilmes, S., Emmons, L. K., and Schichtel, B. A.: How emissions,
527 climate, and land use change will impact mid-century air quality over the United States: a focus on effects at
528 national parks, *Atmos Chem Phys*, 15, 2805-2823, 2015.

529 Wittig, V. E., Ainsworth, E. A., and Long, S. P.: To what extent do current and projected increases in surface
530 ozone affect photosynthesis and stomatal conductance of trees? A meta-analytic review of the last 3 decades of
531 experiments, *Plant Cell Environ*, 30, 1150-1162, doi:10.1111/j.1365-3040.2007.01717.x, 2007.

532 Wu, S., Mickley, L. J., Kaplan, J. O., and Jacob, D. J.: Impacts of changes in land use and land cover on
533 atmospheric chemistry and air quality over the 21st century, *Atmos Chem Phys*, 12, 1597-1609,
534 doi:10.5194/acp-12-1597-2012, 2012.

535 Yue, X., and Unger, N.: Ozone vegetation damage effects on gross primary productivity in the United States,
536 *Atmos Chem Phys*, 14, 9137-9153, doi:10.5194/acp-14-9137-2014, 2014.

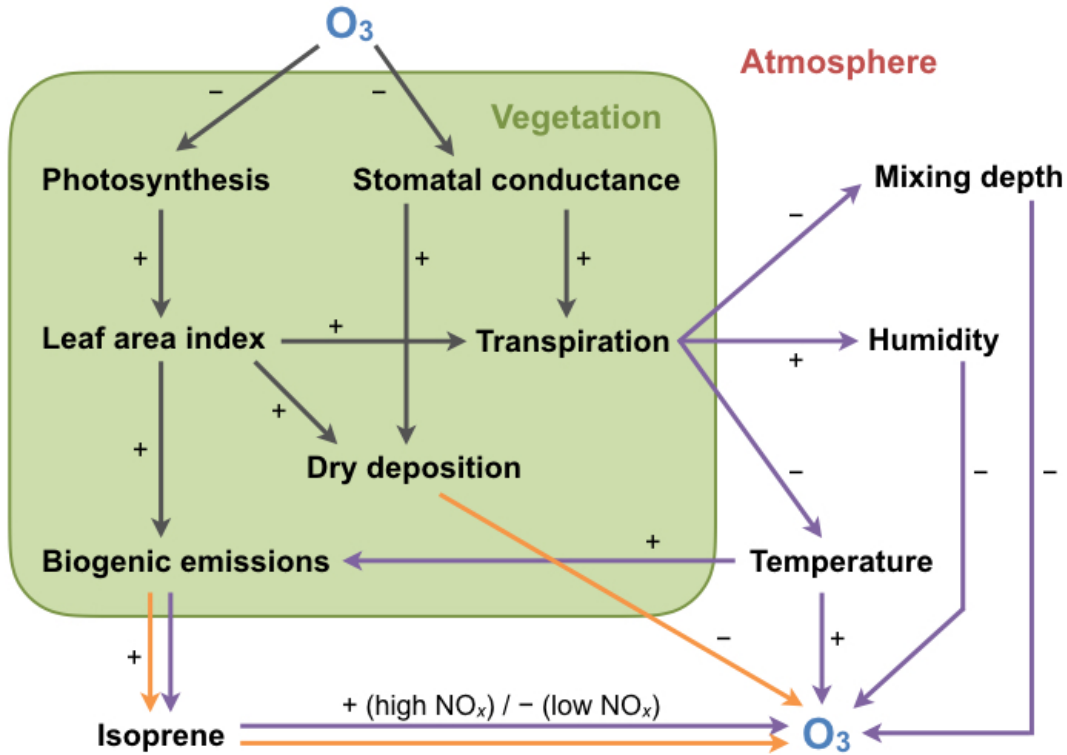
537 Yue, X., and Unger, N.: The Yale Interactive terrestrial Biosphere model version 1.0: description, evaluation and
538 implementation into NASA GISS ModelE2, *Geosci Model Dev*, 8, 2399-2417, doi:10.5194/gmd-8-2399-2015,
539 2015.

540

541 Table 1. Slopes (per mmol m^{-2}) and intercepts (unitless) used to calculate ozone impact
542 factors in Eq. (4) and (5), following Lombardozzi et al. (2015).
543

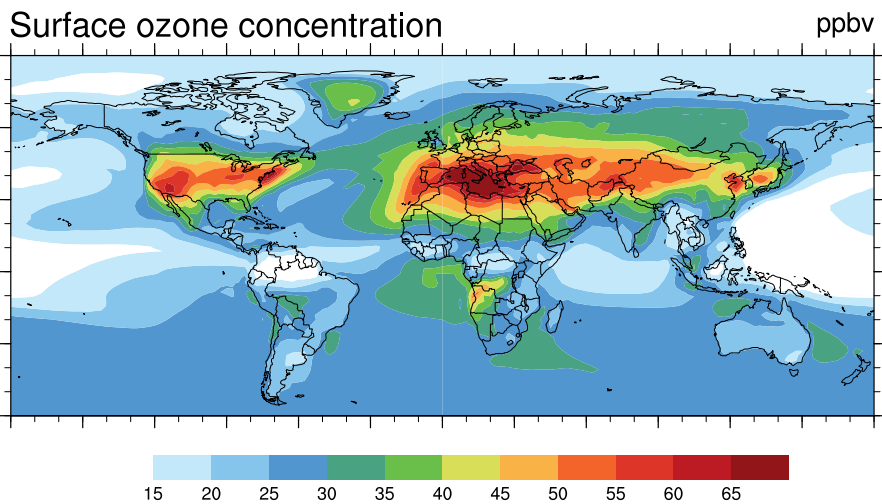
Plant group	Photosynthesis		Conductance	
	Slope (a_p)	Intercept (b_p)	Slope (a_c)	Intercept (b_c)
Broadleaf	0	0.8752	0	0.9125
Needleleaf	0	0.839	0.0048	0.7823
Crops and grasses	-0.0009	0.8021	0	0.7511

544



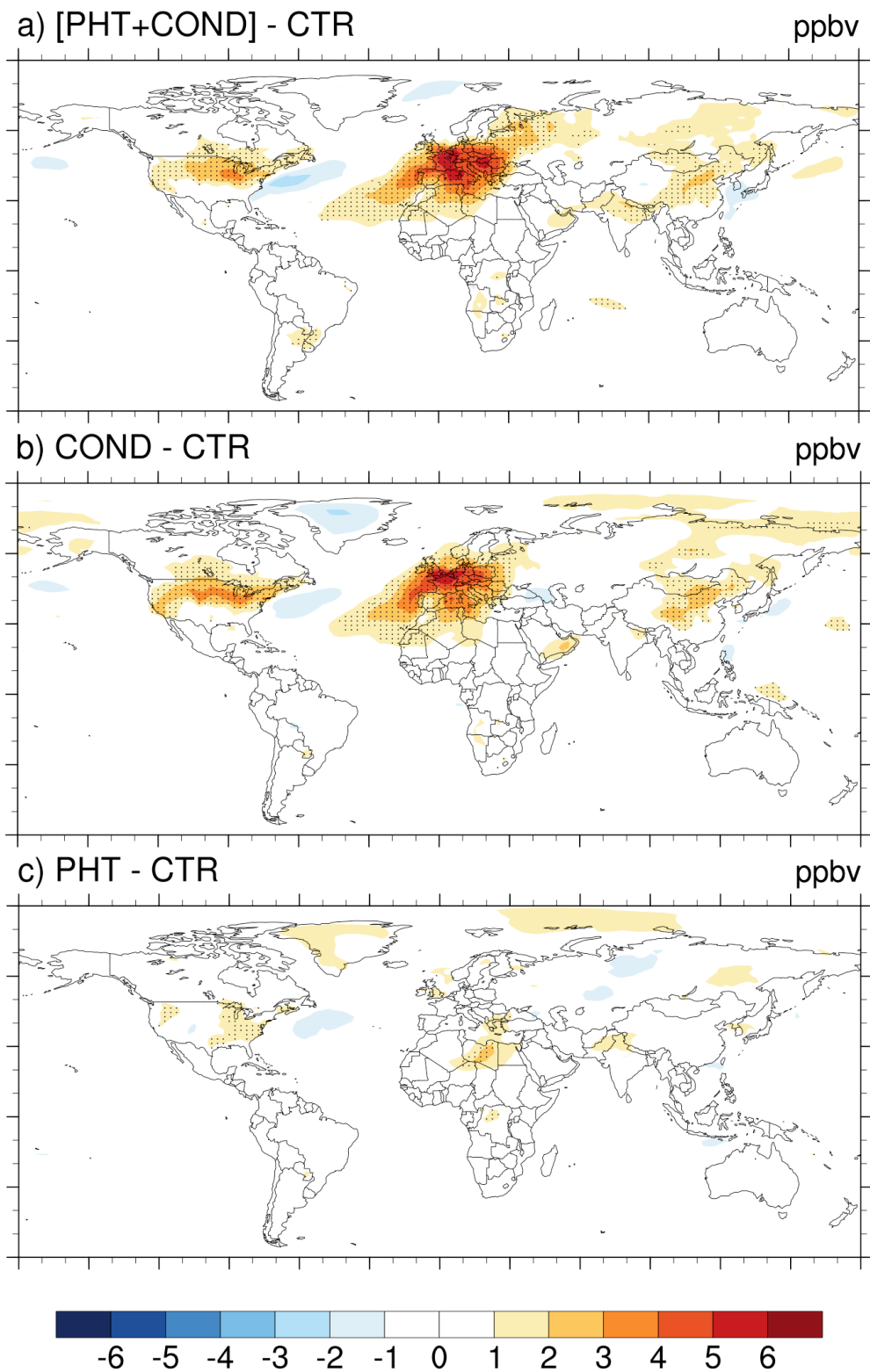
545
546
547
548
549
550
551
552

Figure 1. Possible pathways of ozone-vegetation coupling and feedbacks. The sign on each arrow indicates the sign of correlation or effect of one variable with or on another variable; the product of all signs along a given pathway indicates the overall sign of feedback. Orange arrows indicate biogeochemical feedbacks (i.e., via modulating atmospheric chemistry directly); purple arrows indicate meteorological feedbacks (i.e., via modifying the hydrometeorological environment). We focus only on processes that directly affect ozone; meteorological feedbacks on photosynthesis and stomatal conductance are included in the model but not emphasized in this figure.

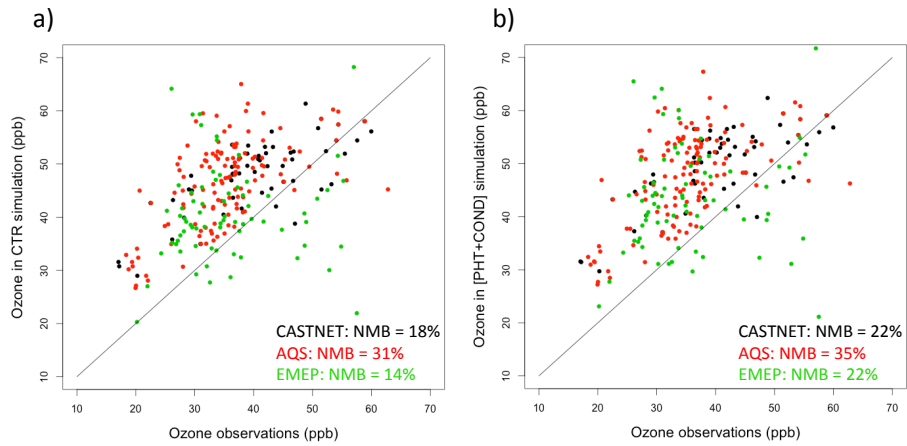


553
554
555
556

Figure 2. Mean summertime (JJA) surface ozone concentration from the [PHT+COND] case, where ozone uptake simultaneously modifies both photosynthetic rate and stomatal conductance. Results are averaged over the last 15 years of simulations.



557
 558 Figure 3. Changes in summertime surface ozone concentrations in different simulations: (a) the case where both
 559 photosynthetic rate and stomatal conductance are modified by ozone uptake; (b) modified photosynthetic rate only; and (c)
 560 modified stomatal conductance only, all relative to the control case (CTR). Stippling with dots indicates significant changes
 561 at 90% confidence from Student's *t* test.
 562



563

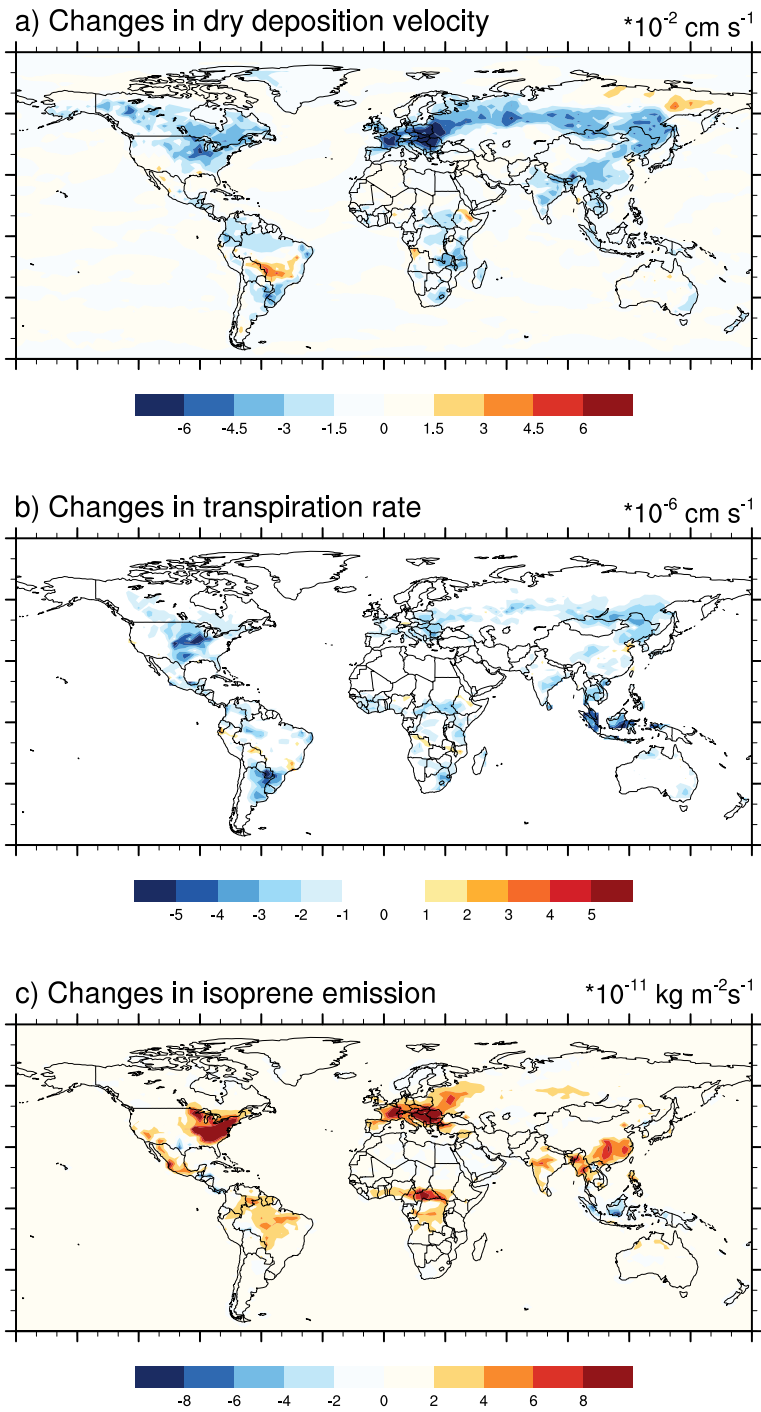
564

Figure 4. Scatterplots of simulated summertime ozone concentration in (a) the control case (CTR); and (b) the case where both photosynthesis and conductance are modified by ozone uptake ([PHT+COND]), versus observed average values from the Clean Air Status and Trends Network (CASTNET) (1999-2001), Air Quality System (AQS) (1999-2001), and European Monitoring and Evaluation Programme (EMEP) (1999-2001). Normalized mean biases (NMB) are also shown.

565

566

567

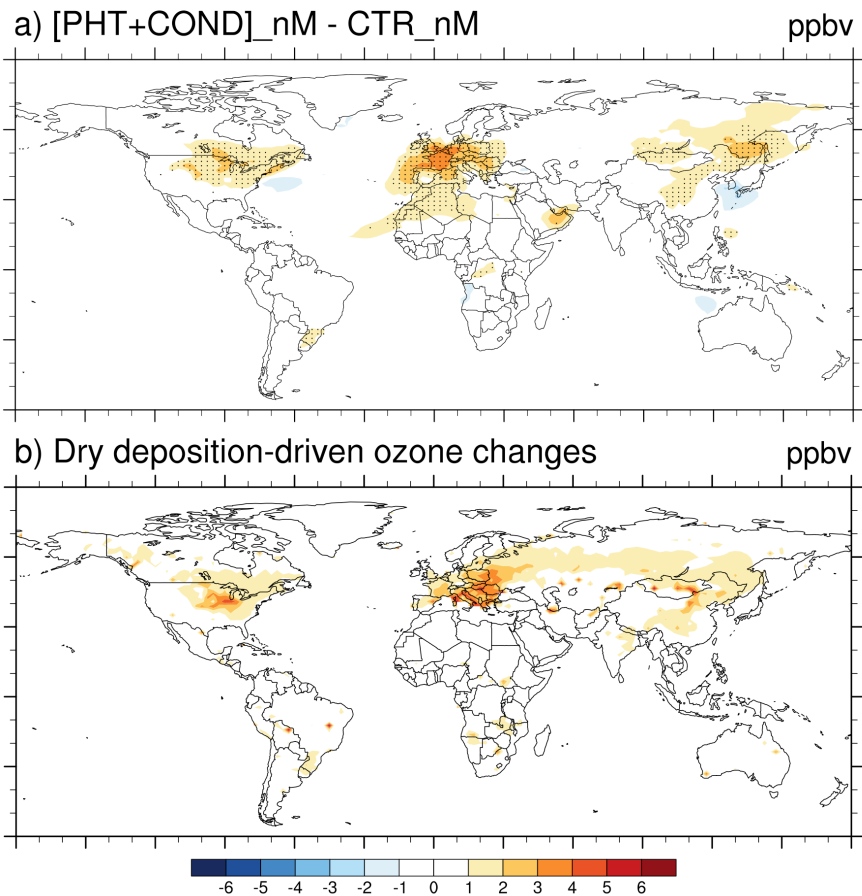


568

569

570

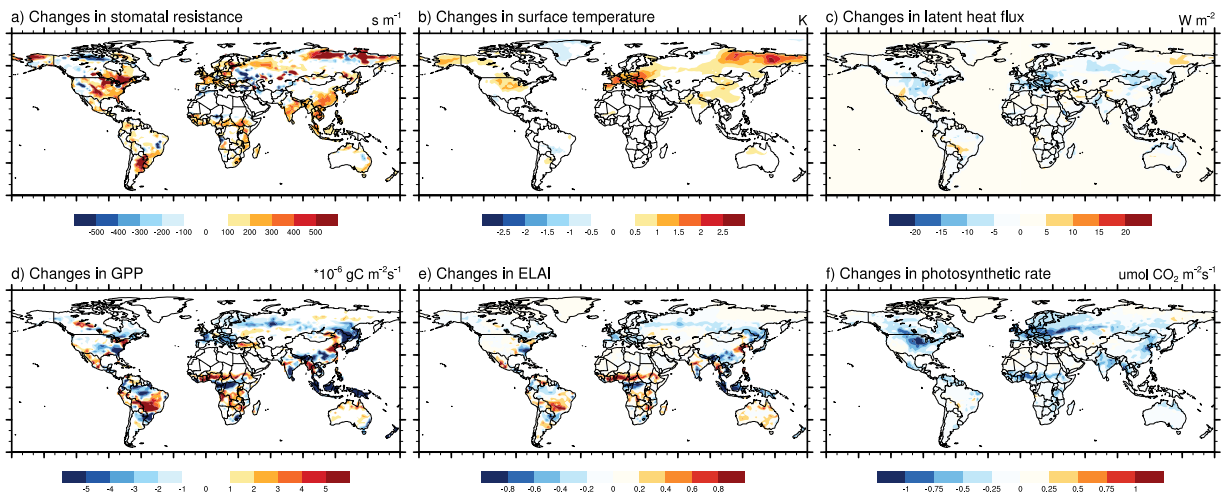
Figure 5. Changes in (a) dry deposition velocity, (b) transpiration rate and (c) isoprene emission in the [PHT+COND] case, where both photosynthetic rate and stomatal conductance are modified by ozone uptake, relative to the control case (CTR).



571
572
573
574
575
576
577

Figure 6. Changes in surface ozone concentration in: (a) the case where both photosynthesis and stomatal conductance are modified by ozone uptake, but with prescribed isoprene emission from the original control case (CTR) by turning off MEGAN (stippling with dots indicates significant changes at 90% confidence from Student's *t* test); and (b) theoretical changes calculated by multiplying our simulated dry deposition changes with the change in ozone concentration per unit change in dry deposition from Val Martin et al. (2014), which did not include ozone damage on vegetation.

578



579

580

581

582

Figure 7. Changes in (a) stomatal resistance, (b) surface temperature, (c) latent heat flux, (d) gross primary production (GPP), (e) effective leaf area index (ELAI) and (f) photosynthetic rate in the [PHT+COND] case, where both photosynthetic rate and stomatal conductance are modified by ozone uptake, relative to the control case (CTR).